quantum reports

MDPI

Article

Vacuum Fluctuations as the Stiffness of Spacetime: Induced Regge Gravity on the Selection–Stitch Lattice

Raghu Kulkarni

SSMTheory Group, IDrive Inc., Calabasas, CA 91302, USA; raghu@idrive.com

Abstract

The gravitational sector of the Selection–Stitch Model (SSM) is Regge calculus on the D_4 lattice, with its action assumed. We derive it from the vacuum fluctuations of quantum fields. If the fluctuations are regulated covariantly on the piecewise-flat geometry of the lattice's edge lengths, integrating them out induces the Einstein–Hilbert term, which, on that geometry, is exactly the Regge action. The conical heat-kernel coefficient, computed from the exact spectrum of a cone, gives the hinge action $-(8\pi G_{\mathrm{ind}})^{-1} A\delta\,[1+\delta/4\pi+O(\delta^2)]$; intersecting hinges enter only at lower powers of the cutoff. Lattice-regulated fields instead give the graviton a mass, even with their cutoff softened below the lattice scale. A defect's verification cost, counted in proper-time ticks, couples as a rest mass and sources Einstein's equation. The induced Newton constant is $1/G_{\mathrm{ind}} = C\Lambda^2/12\pi$. With the cutoff fixed by mode counting, the SSM's area-law G requires $C = 4.2$–5.9; three generations of the Spin(10) spinor with the Standard Model gauge group and a minimal Higgs give $C = 4$, a near-cancellation that survives a mismatch of the fermion and gauge-field cutoffs between -1% and $+5\%$. Requiring the two values of G to agree admits right-handed neutrinos and excludes supersymmetry and Higgs inflation. The covariance of the fluctuations is assumed, not derived from the lattice, and the treatment is Euclidean and one-loop.

Keywords: induced gravity; Regge calculus; heat kernel; conical singularity; vacuum fluctuations; D_4 lattice; Newton's constant

1. Introduction

In the Selection–Stitch Model (SSM), the structure of spacetime is a lattice of Planck-scale bonds, face-centered cubic in space and the D_4 root lattice in four dimensions, on which a quantum error-correcting code runs [1,2]. Matter is a defect of that lattice, and mass is the cost of verifying it [2]. Gravity is the Regge calculus of the lattice's edge lengths [3]: curvature sits on the triangular hinges, and the action is $S = -(8\pi G)^{-1}\sum_\sigma A_\sigma \delta_\sigma$. On the closed D_4 complex, this action reproduces the Fierz–Pauli and Einstein–Hilbert terms exactly at two derivatives, and its field equations give the Newtonian limit and post-Newtonian $\beta = \gamma = 1$ [4]. In that work, as in almost all of Regge calculus, the action itself is assumed.

This paper derives it. The proposal is physical before it is technical: the lattice and its defects float on the vacuum's fluctuations, and gravity is the stiffness those fluctuations give to space, in the sense of Sakharov's induced gravity [5,6]. Section 2 reviews the measured fluctuations and states the SSM's premise about them, the saturation rule that keeps them from creating new space, and the covariance postulate the derivation of the action uses. Section 3 explains why they cannot be the lattice's own fields. Section 4 derives the Regge action and its source, Section 5 computes Newton's constant and compares it

Check for updates

Academic Editor: Gerald B. Cleaver

Received: 25 September 2026
Revised: 20 October 2026
Accepted: 22 October 2026
Published: 26 October 2026

Copyright: © 2026 by the author. Licensee MDPI, Basel, Switzerland. This article is an open access article distributed under the terms and conditions of the Creative Commons Attribution (CC BY) license.

with the SSM's independent area-law value, and Sections 6 and 7 collect consistency checks and limitations.

What is new.

Sakharov's mechanism itself is standard. This paper adds four things. It shows that the fluctuations inducing the lattice's dynamics cannot be the lattice's own fields: every lattice-regulated sector we test, including those priced by the SSM's error-correction costs, gives the graviton a mass (Section 3). It verifies the Regge hinge term directly on the conical singularity, from an exact spectrum, rather than through the smooth-curvature identity alone (Section 4.3). It derives the source: a defect's verification cost, counted in proper-time ticks, couples to the geometry as a rest mass, which gives the equivalence principle and makes verification cost the source of curvature (Section 4.5). And it tests the induced Newton constant against the SSM's independent area-law value, with a cutoff fixed by mode counting rather than chosen (Section 5); read the other way, the agreement becomes a budget on all fields below the Planck scale, with falsifiable consequences for particle physics (A Gravity–Content Budget Section).

Scope of the claims.

The derivation of the Regge action is conditional on Postulate 2, the covariance of the vacuum fluctuations, and that of the source on Postulate 3; everything after them is an exact identity, a standard heat-kernel result, a counting argument, or a computation reported with its numerics. Postulate 1, that the fluctuations predate spacetime, frames the model but is not used in either derivation. The comparison of G is an order-one test under two stated cutoff schemes, not a precision prediction. The induced-action computations are Euclidean and one-loop. The paper does not supply a dynamical mechanism for the covariance of the fluctuations, a Lorentzian or higher-loop treatment, a solution of the cosmological-constant problem, or the dynamics of vacancy boundaries; Section 7 states how each bears on the results. A status table there grades every claim.

2. The Ocean and the Lattice

The ocean is observed.

The ground state of a quantum field is not empty: its field values fluctuate at every wavelength. The fluctuations were first inferred from their effects, the Lamb shift of hydrogen [7,8], read by Welton as the jitter of an electron in the vacuum field [9], and the Casimir force between conductors [10]. They are now measured directly: the electric field of the vacuum has been sampled in time [11], its correlation spectrum measured [12], and its correlations detected between points outside each other's light cone [13], and moving boundaries convert them into real photons [14]. Whether the fluctuations should be called virtual particles is an interpretive question [15]; their existence and spectrum are not. We call them the ocean.

Postulate 1 (The ocean)**.** *The vacuum fluctuations predate the lattice, and with it spacetime, and persist in it. They are the substrate from which the lattice's bonds and its defects formed.*

Postulate 1 is an interpretive premise of the SSM, not a testable hypothesis, and we do not present it as one. No result below uses it: every derivation needs only that quantum fields fluctuate on the lattice's geometry today, which is measured. Dropping Postulate 1 removes the account of Section 2's next paragraph and changes no equation, table, or figure.

https://doi.org/10.3390/quantum8040109

Before the lattice.

The SSM's account of what precedes the lattice is the following. Before there is a lattice, there are only these fluctuations: degrees of freedom defined by their algebra alone, with no position, since location is a lattice property. Among all possible rulebooks, the one realized is one in which some structure can persist; quantum theory is the natural candidate, because it permits relation without prior geometry (entanglement), combines variation with heredity, and supports self-verification. The first persistent structure is the smallest closed cycle of verified relation, three degrees of freedom pairwise entangled: the triangle. Adjacency is verified relation, so the triangle is the first geometry and its verification cycle is the first clock. From it, the SSM's crystallization proceeds as published: the triangle seed grows into a two-dimensional sheet, lifts into three dimensions, and completes the transition to the close-packed lattice, trapping the remnant nodes that are matter [2]. The lattice that emerges is polycrystalline even from a single seed: its bulk is FCC, and the interior nodes short of full coordination sit at $K = 10$–11, on the boundaries between crystallites of different orientations [2]. The lattice and its defects are both made of stitched fluctuations.

After the lattice: The saturation rule.

Stitching converts fluctuations into bonds but does not exhaust them; the ocean persists around the finished lattice and its defects. It does not keep creating space, and the reason is the rule that created space in the first place. A bond forms only where a node can accept one, and a node already surrounded by the maximal number of neighbors at bond distance cannot: that maximum is the kissing number, 12 in three dimensions [16] and 24 in four [17], which the FCC slice and the D_4 lattice attain. The SSM's growth kinematics applies exactly this rule [2]. Away from defects and grain boundaries, every node is saturated, so the ocean cannot stitch there: the existing lattice excludes new bonds at the points it already occupies. Stitching remains possible only where coordination is incomplete: at growth fronts, at the grain boundaries between crystallites, and at the boundaries of vacancies, where it would compete with a vacancy's evaporation [18]. We do not treat that competition here. The ocean therefore coexists with space rather than adding to it. Once space exists, the persisting fluctuations are the field modes on its geometry, and so acquire location from it; the measured vacuum fluctuations above are this present-day remainder.

The covariance postulate.

Two further properties of the ocean matter for gravity: it has no rest frame, and it sees the lattice as geometry. The measured correlations of the vacuum field outside the light cone [13] are those of the Lorentz-invariant vacuum of quantum field theory, and are consistent with the first. We state both together.

Postulate 2 (Covariant ocean)**.** *The persisting vacuum fluctuations are those of quantum fields coupled to the piecewise-flat geometry defined by the lattice's edge lengths, minimally unless stated otherwise, and regulated covariantly, by a proper-time cutoff Λ that respects the symmetry of the geometry rather than that of the lattice. The scale of Λ is set by the lattice's mode density (Section 5).*

Covariance is what makes the ocean frictionless and non-dissipative for matter in uniform motion: a Lorentz-invariant vacuum is a pure state with no preferred frame, so a uniformly moving body cannot detect its motion through it, and there is no bath to decohere into. Accelerated motion does couple to the vacuum (the Unruh effect), as it must. Postulate 1 is the model's premise; Postulate 2 is the assumption the derivation of the Regge action uses, and Section 3 shows that it cannot be weakened to fields regulated by the lattice itself. A third postulate, for the source, is stated in Section 4.5.

What the covariance postulate requires, and what it does not.

A discrete lattice and a covariant regulator can appear to contradict each other. Five points locate exactly what Postulate 2 asks for. (i) What is discrete is the geometry's degrees of freedom, the edge lengths, not the space the fluctuations live on. A piecewise-flat geometry is a continuous manifold with a metric that is flat in every four-simplex, and fields on it, with their covariant heat kernel, are well defined; this is the setting in which Cheeger, Müller, and Schrader proved that the heat-kernel curvature of piecewise-flat spaces is Regge's [19,20]. Inside each simplex, the metric is exactly flat, so a proper-time regulator there is the flat-space one and is unambiguous; the only place where the discrete geometry and the regulator meet is the hinges, which Section 4.3 treats exactly. (ii) The regulator does not regulate the code. The stabilizer sector contributes nothing to the induced action for any couplings (Section 3), so the code's discrete structure, including its cluster and locality properties, never enters the fluctuation determinant, and the postulate places no demand on it. (iii) Discreteness does not by itself select a frame. Lorentz-invariant discreteness exists: no equivariant rule can assign a preferred direction to a Poisson sprinkling of Minkowski space [21]. A regular lattice does break boosts, and in the SSM, it does so only through its geometry, at relative order $(E/E_{\mathrm{P}})^2$ (Section 6); the postulate is that this breaking is not transmitted to the fluctuations' regulator. (iv) The direction of the scale-setting can be reversed. In the SSM, the bonds are made of the fluctuations (Postulate 1), so the lattice spacing would be set by the fluctuations' short-distance scale rather than the regulator by the lattice; mode counting (Section 5) then fixes the ratio of the two scales, not their origin. This reading is offered as an interpretation. (v) The distinction between covariant and lattice-regulated fluctuations is not introduced to evade the no-go of Section 3; it is decided by observation. Lattice-regulated fluctuations give the graviton a mass of order the cutoff, while gravitational-wave propagation bounds it below $1.27 \times 10^{-23}\,\mathrm{eV}/c^2$ [22], and softening their cutoff below the lattice scale reduces the mass only as a power of the cutoff (Section 3), so covariance must hold exactly rather than approximately. What remains unexplained is the mechanism: the paper does not derive covariance from the lattice, and we list this as its principal open problem (Section 7).

3. Why the Fluctuations Cannot Be the Lattice's Own

Two results close the alternative in which the lattice's own sectors induce its dynamics.

The stabilizer sector induces nothing.

The code's check Hamiltonian is $H = \sum_i J_i(1 - S_i)/2$, where the checks S_i are commuting Pauli products with eigenvalues ± 1. Each term is non-negative, and all terms vanish on the code space, where every $S_i = +1$; the code space is nonempty because the checks form a valid CSS stabilizer group [1]. The ground energy is therefore exactly zero for every choice of positive couplings J_i, and the ground space does not depend on them. However the couplings are made to depend on the edge lengths, neither changes, so the pure code contributes no induced action, curvature term or otherwise. This survives dynamical perturbations of the metric. If the couplings fluctuate, whether as time-dependent functions $J_i(\ell(t))$ or as operators $J_i(\hat{\ell})$ acting on the geometry's degrees of freedom, the Hamiltonian is $\sum_i J_i \otimes (1 - S_i)/2$ and still annihilates every state of the form $|\mathrm{code}\rangle \otimes |\mathrm{geometry}\rangle$. The projector onto the code space is independent of the couplings, so there is no Berry phase, no adiabatic excitation, and no geometry-dependent ground energy. The argument requires only that each J_i stay positive, which a small metric perturbation cannot reverse. With the other sign convention, $H' = -\sum_i J_i S_i$, the ground energy is $-\sum_i J_i$: an ultralocal sum of one term per check, which depends on the edge lengths only through each check's own

couplings and contains no deficit angles, so it is not a curvature term either. Vacuum fluctuations, and with them any induced gravity, come only from non-commuting dynamics.

Lattice-regulated fields give the graviton a mass.

For the dynamical sectors, we computed the one-loop vacuum energy $W(\epsilon)$ of fields living on the D_4 lattice under a uniform strain $g = 1 + \epsilon$, with bond couplings depending on bond lengths. A uniform strain is a flat geometry in other coordinates, so the Regge action gives it zero cost for any shape; an induced action compatible with Regge must depend on it only through the volume. If W depends on ϵ only through $\sqrt{\det g}$, its gradient at $\epsilon = 0$ is $\frac{1}{2} w\, \delta_{\mu\nu}$, which defines the volume response w, and its second derivative along any traceless unit direction is $-\frac{1}{2} w$. The test is therefore the shape (traceless) response of W against $-\frac{1}{2} w$, and it suffices at $k = 0$: no term at $O(k^2)$ can repair a shape dependence of the uniform vacuum energy. Couplings are priced in two ways suggested by the SSM's error-correction costs, with each bond's quantum costing $\hbar c/4\ell$: per bond, $J_e \propto 1/\ell_e$ (for a gauge plaquette, the mean of $1/\ell$ over its three bonds); and per check support, $J \propto 1/\bar{\ell}$ with $\bar{\ell}$ the mean bond length of the check (a vertex star, or a plaquette). Table 1 lists the ratio of the measured shape response to the covariant value.

Table 1. Shape response of the induced vacuum energy of lattice-regulated fields under uniform strain, relative to the covariant value (covariance requires 1). QEC: Error-correction. The gauge field lives on the root links with root-triangle plaquettes. For the scalar, all nine traceless directions give the same value, and for the other fields, every direction tested does, as the rank-four isotropy of D_4 requires. Momentum grids 16^4 and 24^4 (scalar, Dirac, control) and 8^4 and 12^4 (gauge) agree to four digits. The Wilson–Dirac operator is $D(k) = \sum_j t_j \left[(\gamma \cdot \hat{n}_j)\, e^{ik \cdot d_j} + r\,(1 - \cos k \cdot d_j) \right]$, summed over the 24 root vectors d_j with $\hat{n}_j = d_j/|d_j|$ and bond amplitudes t_j, including a Wilson term [23] that gaps the doublers; the ratio shown is at $r = 1$ and lies between 0.49 and 0.56 for $0.25 \le r \le 4$.

Bond Couplings	Real Scalar	U(1) Gauge	Wilson–Dirac
QEC pricing per bond ($J \propto 1/\ell$)	0.492	0.475	0.500
QEC pricing per check support	0.167	0.253	0.167
exact continuum kinetic tensor	0.143	–	–

Every coupling rule fails, including one built to reproduce the continuum kinetic tensor exactly. A shape-dependent vacuum energy is an induced shear stiffness at the lattice scale, which gives the graviton a mass of order the cutoff. The same holds for any energy that depends on the shape of a uniform strain, including an elastic energy intrinsic to the lattice, which is why the lattice can have no appreciable stiffness of its own (Section 4.4); for the bosonic fields, the induced stiffness is negative, so it would also destabilize the lattice against shear. For a power-law coupling $J \propto \ell^{-p}$, covariance is restored only at a field-dependent exponent, $p^* = 4.1996$ for the scalar and 4.6899 for the gauge field, so no single rule works. Because the shape excess is close to $\frac{1}{4} w$ for every species, bosonic and fermionic fields cancel it approximately when their lattice mode counts balance, but only to a few percent. The obstruction is generic: the modes near the lattice cutoff see the crystal's shape. Postulate 2 removes it by construction, since a covariantly regulated ocean has no preferred shape.

Softening the cutoff does not restore covariance.

One might hope that lattice fields become covariant if their modes are cut off smoothly below the lattice scale, so that only long wavelengths, which see the continuum, contribute. We tested this in the most favorable case: a scalar on the D_4 vertices whose couplings reproduce the continuum kinetic tensor $6\sqrt{g}\, g^{-1}$ exactly, so that every departure from covariance comes from short-distance lattice structure, regulated by the same proper-time

cutoff as Equation (1), now applied to the lattice operator, $W = \frac{1}{2}\langle E_1(\mathcal{D}_q/\Lambda^2)\rangle$ with $\mathcal{D}_q$ the lattice Laplacian. Table 2 gives the relative shape excess $\Delta_{\rm sh}$, the shape response divided by its covariant value, minus one. It falls as the cutoff is lowered, but only as a power, $\Delta_{\rm sh} \simeq 0.029\,(\Lambda L_f)^2$, because the lattice dispersion departs from the continuum at relative order $(qa)^2$ at every momentum. A shape excess is a Fierz–Pauli-violating mass term; for one field, with G from the area law, $m_g L_f \simeq (\Lambda L_f)^2[\Delta_{\rm sh}/(16\pi \ln 2)]^{1/2}$. The gravitational-wave bound then requires $\Lambda L_f \lesssim 4 \times 10^{-17}$, where the induced Newton constant would exceed the area-law value by a factor of order 10^{34}; equivalently, bosonic and fermionic excesses would have to cancel to roughly one part in 10^{100}. Approximate covariance therefore does not suffice: the shape response must vanish exactly, which no lattice-regulated sector we have tested achieves at any cutoff. This is why Postulate 2 requires the fluctuations' short-distance completion to be covariant in its own right rather than inherited from the lattice (`soft_cutoff_covariance.py`).

Table 2. Lattice-regulated scalar with the exact continuum kinetic tensor and a smooth proper-time cutoff Λ: relative shape excess $\Delta_{\rm sh}$ of the induced vacuum energy under uniform strain (zero for a covariant field), and the graviton mass it implies for one field, with $L_f = \sqrt{4\ln 2}\,\ell_{\rm P}$. Observation requires $m_g < 1.27 \times 10^{-23}$ eV.

ΛL_f	$\Delta_{\rm sh}$	$m_g L_f$	m_g (eV)
0.5	0.0071	0.0036	3×10^{25}
0.8	0.019	0.015	1×10^{26}
1.0	0.038	0.033	2×10^{26}
2.0	0.54	0.50	4×10^{27}
4.22 (mode count)	0.79	2.7	2×10^{28}

4. Derivation of the Regge Action and Its Source

4.1. Sakharov's Mechanism

For a field with Laplace-type fluctuation operator $\mathcal{D} = -(\nabla^2 + E)$, the one-loop Euclidean effective action with proper-time cutoff Λ is

$$\Gamma = -\frac{s}{2}\int_{\Lambda^{-2}}^{\infty}\frac{dt}{t}\,\mathrm{Tr}\,e^{-t\mathcal{D}}, \qquad \mathrm{Tr}\,e^{-t\mathcal{D}} = \frac{1}{(4\pi t)^2}\int\sqrt{g}\,\big[a_0 + t\,a_1 + t^2 a_2 + \dots\big], \tag{1}$$

where t is the proper-time (Schwinger) parameter, Tr the functional trace over the field's components, Λ the cutoff, a_k the heat-kernel coefficients, and s the statistics sign: $s = +1$ for bosons and $s = -1$ for fermions, whose determinant enters the effective action with the opposite power (for which $\mathcal{D} = D'^2$). The first coefficient is $a_1 = \mathrm{tr}(E + R/6)$ [24]. The a_0 term is a cosmological term of order Λ^4; the a_1 term is

$$\Gamma \supset -\frac{C\,\Lambda^2}{192\pi^2}\int\sqrt{g}\,R \equiv -\frac{1}{16\pi G_{\rm ind}}\int\sqrt{g}\,R, \qquad \frac{1}{G_{\rm ind}} = \frac{C\,\Lambda^2}{12\pi}, \tag{2}$$

where C counts the fields in units of a minimally coupled real scalar. From the coefficients a_1 of each species (Appendix A),

$$C = N_s(1 - 6\xi) + N_{\rm Weyl} + 2N_{\rm Dirac} - 4N_V, \tag{3}$$

with ξ the scalar curvature coupling and N_V the number of gauge fields. Minimally coupled scalars and fermions induce a positive Newton constant, a conformally coupled scalar ($\xi = \frac{1}{6}$) none, and gauge fields a negative one. This is Sakharov's "metrical elasticity of space" [5], here supplied by the vacuum fluctuations; the curvature-squared terms a_2 are logarithmic in Λ and suppressed at long wavelength.

4.2. The Lattice as Piecewise-Flat Geometry

The SSM's edge lengths define a piecewise-flat geometry: flat inside every four-simplex, with curvature concentrated on the triangular hinges. For such a geometry, the Einstein–Hilbert integral is exactly [3,19]

$$\int \sqrt{g}\, R = 2 \sum_{\sigma} A_\sigma\, \delta_\sigma, \tag{4}$$

where A_σ is the area of hinge σ and δ_σ its deficit angle. Substituting Equation (4) into Equation (2) gives the Regge action with Newton's constant G_{ind}. Because a piecewise-flat geometry is singular at the hinges, we verify this step directly on the singularity.

4.3. The Hinge Term from the Conical Heat Kernel

Near a hinge, the geometry is a flat plane times a two-dimensional cone of angle $2\pi\alpha$, with $\delta = 2\pi(1-\alpha)$. The heat-kernel trace on a cone carries a vertex term beyond the smooth expansion. For a scalar, it is [20,25]

$$\mathrm{Tr}\, e^{-t\mathcal{D}}\big|_{\mathrm{vertex}} = \frac{1}{12}\left(\frac{1}{\alpha} - \alpha\right), \tag{5}$$

independent of t, and in four dimensions, the hinge contributes $A_\sigma (4\pi t)^{-1}$ times this. We verify Equation (5) independently of the literature. For a cone-disk of radius 1 and angle $2\pi\alpha$ with a Dirichlet boundary, the spectrum is $j_{\nu,k}^2$ with $\nu = |m|/\alpha$, the zeros of the Bessel functions J_ν. We compute it exactly, form the heat trace, remove the area and perimeter terms of the Weyl expansion, and fit the constant, which must equal the boundary term $\alpha/6$ plus the vertex term. Figure 1a and Table 3 show the result: the vertex coefficient agrees with Equation (5) to six digits at every cone angle tested, from a deficit of 7.2° to 240°, and the flat disk returns the boundary value $1/6$ exactly.

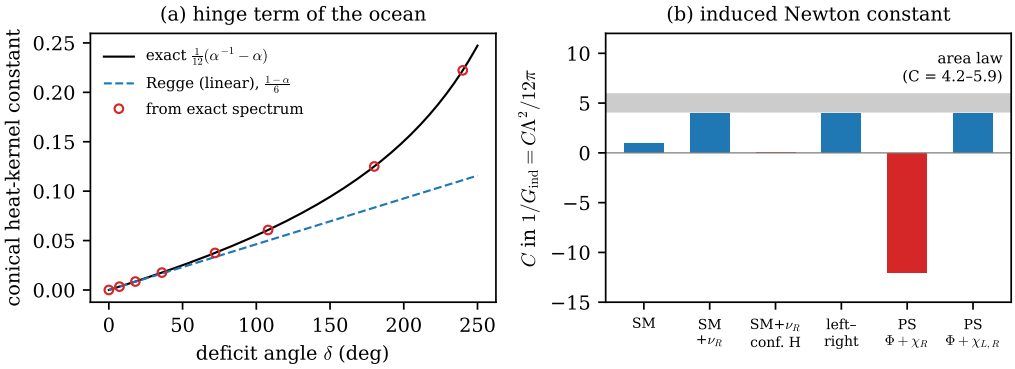


Figure 1. (**a**) The hinge term of the ocean: the conical heat-kernel coefficient from the exact spectrum (circles), the closed form, Equation (5), and its linear part, which is the Regge term. (**b**) The induced Newton constant, Equations (2) and (3), for candidate field contents, against the range the SSM's area law requires under the two mode-count cutoffs (shaded).

Inserting the vertex term into Equation (1) gives, per hinge,

$$\Gamma_\sigma = -\frac{\Lambda^2}{96\pi} A_\sigma \left(\frac{1}{\alpha} - \alpha\right) = -\frac{1}{8\pi G_{\mathrm{ind}}} A_\sigma\, \delta_\sigma \left[1 + \frac{\delta_\sigma}{4\pi} + O(\delta_\sigma^2)\right], \tag{6}$$

written for one minimally coupled scalar and normalized with its contribution to G_{ind}. The linear term is the Regge action, with the same G_{ind} as Equation (2); this is the content of Equation (4) on the singularity itself. For every species, the linear term is fixed by its

smooth coefficient a_1, because a cone with a small deficit can be smoothed into a regular geometry with $\int \sqrt{g}R = 2A\delta$ [26]. This includes the curvature couplings in E, which, on the regularized cone, are supported at the tip; for a gauge field, this tip term is the contact term found by Kabat [27], and with it the conical and smooth coefficients agree. The $O(\delta^2)$ corrections are species-dependent curvature-squared terms.

Table 3. Conical vertex coefficient from the exact Bessel spectrum of a cone-disk, against the closed form, Equation (5), and its linear (Regge) part $(1-\alpha)/6$. The ratio is $(1+\alpha)/2\alpha = 1+\delta/4\pi+O(\delta^2)$.

α	δ	Vertex, Numerical	$\frac{1}{12}(\alpha^{-1}-\alpha)$	Linear (Regge)	Ratio
0.98	7.2°	0.003367	0.003367	0.003333	1.010
0.95	18°	0.008553	0.008553	0.008333	1.026
0.90	36°	0.017593	0.017593	0.016667	1.056
0.80	72°	0.037500	0.037500	0.033333	1.125
0.50	180°	0.125000	0.125000	0.083333	1.500

Where hinges meet.

The cone computation treats an isolated hinge. On the lattice, hinges meet along edges and at vertices, and the cutoff length $\Lambda^{-1} \simeq L_f/5$–$L_f/4.2$ (Section 5) is not far below the lattice spacing, so the regions in which neighboring hinges modify the heat kernel overlap. Three facts fix what the overlap can and cannot change.

First, the term linear in the curvature is exact. In covariant perturbation theory, the heat trace is an expansion in powers of the curvature with nonlocal form factors, and its first-order term is $(4\pi t)^{-2}\, t \int \sqrt{g}\, \mathrm{tr}\, P$, with $P = E + R/6$, carrying no form factor at any t [28]. Overlap concerns how the curvatures at different points combine, so it first appears at second order, in products $\delta_\sigma \delta_{\sigma'}$ of the deficits of different hinges. The linear term, which is the Regge term, is not renormalized by it, whatever the ratio of Λ^{-1} to the lattice spacing.

Second, the cutoff dependence is organized by the strata of the singular set. Near a stratum of dimension k, a piecewise-flat geometry is exactly a flat $\mathbb{R}^k$ times a metric cone, which has no length scale of its own. Its contribution to the heat trace, after the bulk and lower-codimension terms are subtracted, is therefore its k-volume times $t^{-k/2}$ times a constant fixed by the cone [20]: in four dimensions, the bulk enters at order Λ^4, the hinges ($k=2$) at Λ^2, the edges ($k=1$) at Λ, and the vertices ($k=0$) at $\ln\Lambda$. Cross terms between hinges that share an edge or a vertex are localized there, so they enter at order Λ or $\ln\Lambda$, suppressed relative to the hinge terms by $1/(\Lambda L_f) \approx 0.20$–$0.24$ if their coefficients are of order one, which we have not computed, and, by the first fact, they begin at second order in the deficits. Hinges that share no stratum interact only through terms of order $e^{-(\Lambda d)^2/4}$ at separation d. The coefficient of Λ^2 is therefore exactly $\sum_\sigma A_\sigma \frac{1}{12}(\alpha_\sigma^{-1} - \alpha_\sigma)$, a sum of single-hinge terms.

Third, an exactly solvable case is consistent with this. The flat orbifolds T^4/G with G generated by rotations by π in coordinate planes are piecewise-flat spaces whose hinges, the fixed planes, have $\alpha = \frac{1}{2}$, a deficit of 180°, and intersect: for $G = \langle R_{12}, R_{23}\rangle$, three families of hinges meet along lines and at points, and for $G = \langle R_{12}, R_{34}\rangle$, two families meet at points. Their heat traces follow exactly from the torus spectrum. In both, the Λ^2 coefficient is $\frac{1}{8}$ per unit hinge area, the isolated-cone value $\frac{1}{12}(\alpha^{-1}-\alpha)$, and the strata formula reproduces the trace to 1.5×10^{-7}, the size of the exponential remainder, for $0.004 \le t \le 0.015$ in units of the torus period (`orbifold_hinges.py`). This is a consistency check rather than an independent test: on an abelian orbifold, the image sum makes the hinge terms additive by construction, and orbifold cone angles are restricted to $2\pi/n$. It does confirm the isolated-cone coefficient at intersecting hinges with deficits far larger than those of a weak field.

The intersections therefore affect only the cross terms between hinges, which enter at order Λ, $\ln\Lambda$, and below and depend on how hinges are arranged; the $O(\delta^2)$ self-term of each hinge, $\delta/4\pi$ in Equation (6), is part of the additive Λ^2 coefficient. Both are curvature-squared terms, suppressed at long wavelength since $\delta \sim (ka)^2 h$ for a metric perturbation h of wavenumber k, but at a cutoff this close to the lattice scale, their coefficients carry order-one scheme dependence.

Summing over hinges and species gives the following result.

Proposition 1. *Under Postulate 2, the one-loop action the vacuum fluctuations induce on the SSM lattice is, at leading order in the deficits and the long-wavelength expansion,*

$$S = -\frac{1}{8\pi G_{\text{ind}}} \sum_{\sigma} A_\sigma \, \delta_\sigma, \qquad \frac{1}{G_{\text{ind}}} = \frac{C\Lambda^2}{12\pi}, \tag{7}$$

plus a cosmological term, Section 6, and curvature-squared corrections.

4.4. Two Layers: Discrete Geometry and Continuous Fluctuations

The derivation joins two layers of different character.

The first is the lattice, which supplies spacetime's structure and location. It is discrete: its connectivity is fixed, with every node away from defects and grain boundaries saturated at the kissing number, and its geometry is carried by its edge lengths. Each four-simplex is flat, and curvature is concentrated in deficit angles on the triangular hinges, so curvature is a property of the lengths, not of the connectivity. In the vacuum, every deficit vanishes and the lattice is exactly flat. Near a mass, the edge lengths depart from their vacuum value by an amount of order $GM/(rc^2)$, while no bond is added, removed, or rerouted. In the SSM, a defect's elastic strain energy is negligible compared with its verification cost, so the lattice has no appreciable stiffness of its own, and it must not have one: a stiffness of its own would give the graviton a mass (Section 3).

The second layer is the vacuum fluctuations. They are continuous and carry no structure: they are covariant field modes living on the lattice's piecewise-flat geometry (Postulate 2). They do not bend. Their energy depends on the geometry they live on, and that dependence supplies the stiffness the lattice lacks. The two layers meet at the hinges. Inside each simplex the modes are smooth, but every hinge is a conical singularity, whose vertex term, Equation (5), converts the discrete deficit into its share of the Regge action.

The division of labor is then complete. A defect's mass, its verification cost (Section 4.5), pushes the edge lengths away from flat, producing small deficits on every hinge around it. The fluctuations' energy rises with those deficits, with stiffness $1/G$ set by their content and cutoff. The geometry settles where the two balance, which is Einstein's equation at long wavelength. The response is nonlinear, because the Regge action is nonlinear in the edge lengths, and it is long-ranged, because mass is a conserved source and the covariant fluctuations admit no graviton mass. Structure, and with it error correction, belongs entirely to the lattice; the fluctuations contribute only resistance to its deformation.

Spacetime, in the sense that includes its dynamics, is the two layers together. The lattice's verification cycles supply the ticks of its clocks, but the relative rates of those clocks are set by its geometry, and the geometry is fixed only through the fluctuations' stiffness. The fluctuations also exist where there is no lattice, before crystallization and inside vacancies, so spacetime is made from them rather than they from it.

4.5. The Source: Verification Cost as Rest Mass

The derivation so far fixes the geometry's side of Einstein's equation. Its other side, the source, is a defect's mass, which, in the SSM, is its verification cost [2]: a defect of type

x performs a fixed number C_x of verification operations per tick. We now show that this cost couples to the geometry as a rest mass, with no further assumption about the defect.

In the SSM, time is counted in verification ticks: the triangle's verification cycle is the first clock (Section 2), and every clock since is a count of ticks. In Regge geometry, proper time along a worldline is fixed by the edge lengths it traverses. The one physical input is to identify the two:

Postulate 3 (Ticks are proper time)**.** *The number of verification ticks along a defect's worldline is its proper time in units of a fixed tick duration τ_0, the proper time being the one the lattice's edge lengths assign.*

Postulate 3 is the clock hypothesis of general relativity, that an ideal clock reads proper time along its worldline, applied to the code's verification cycle; like the clock hypothesis, it is assumed. It does not hand-couple the code to an independent geometric layer. The code and the metric live on the same complex: a tick is one update of the D_4 complex, and the proper time a defect accumulates between updates is fixed by the edge lengths of the cells its worldline crosses, which are the metric. What the postulate asserts is that every tick is the same proper time, so that the verification rate per unit proper time is universal. Deriving it would require showing that the edge lengths are themselves fixed by the code's entanglement, so that proper time is a coarse-grained property of the code. The SSM's area law, which ties G to one bit of entanglement per bond cell [18], is a step in that direction, but no such derivation is available, and Postulate 3 remains an input.

Proposition 2. *Under Postulate 3, a defect performing C_x verification operations per tick, each accumulating a fixed phase φ_0, has the Lorentzian worldline action*

$$S_x = -\hbar\varphi_0\, C_x \int \frac{d\tau}{\tau_0} \equiv -M_x c^2 \int d\tau, \qquad M_x c^2 = C_x\, \varepsilon, \quad \varepsilon = \frac{\hbar\varphi_0}{\tau_0}, \tag{8}$$

where φ_0 is fixed by the SSM's calibration of the bond energy. The coupling to the geometry depends on the defect only through M_x, so gravitational and inertial mass are both the verification cost.

The proof is a count. Each verification operation is a step of a quantum process and accumulates a fixed phase φ_0, an action $\hbar\varphi_0$. The number of operations per tick, C_x, is a count and does not depend on the geometry, and by Postulate 3, the number of ticks along a worldline is $\int d\tau/\tau_0$. The action is $\hbar\varphi_0$ times the number of operations, Equation (8). It is the point-particle action of general relativity, and nothing about the defect's internal structure enters it except the count C_x; that is the weak equivalence principle, obtained here from the definition of mass as verification cost rather than assumed. The defect's phase turns at the angular frequency $M_x c^2/\hbar = C_x\varphi_0/\tau_0$: its rate of verification sets its Compton frequency.

In the static weak-field limit, $d\tau = \sqrt{g_{44}}\, dt$, so $S_x \simeq -M_x c^2 \int (1 + \frac{1}{2}h_{44})\, dt$: the defect couples to the geometry through $\frac{1}{2}M_x h_{44}$, which is exactly the source coupling used in Reference [4]. The two actions must be combined in one signature. Equation (8) is the Lorentzian point-particle action; the induced action, Equation (7), is computed in Euclidean signature, where the corresponding matter term is $+M_x c^2 \int ds_x$, with s_x the Euclidean proper time, and the two forms are related by the Wick rotation $t = -it_E$, with $iS^{(L)} = -S^{(E)}$. Varying the induced action together with the matter action, both in the same signature and summed over defects, gives the Regge equations with a source, and at long wavelength Einstein's equation, $G_{\mu\nu} = 8\pi G_{\mathrm{ind}} T_{\mu\nu}$, with $T_{\mu\nu}$ built from the verification-cost density. Two statements follow, and they are the precise sense in which verification cost is proportional to curvature. Locally, for slowly moving defects of cost density ρ, the

time-time Ricci curvature is $R_{tt} = 4\pi G_{\text{ind}}\rho$, the local form of Poisson's equation. Outside the defects, where the cost density vanishes, the tidal curvature is fixed by the total enclosed cost, and on the D_4 lattice, the static field it produces has the Newtonian normalization exactly, with $\beta = \gamma = 1$ at second order [4].

Extended defects.

A defect extends over a few lattice cells; it is not a point. Its internal structure enters the far field only through higher multipoles: the monopole is fixed by the total cost through the Newtonian normalization [4], the dipole vanishes about the center of cost, and the quadrupole is suppressed by $(R/r)^2$ for a defect of size R. Its spin, which the worldline action omits, couples to curvature at relative order $\hbar/(Mcr)$, the ratio of its Compton wavelength to the distance r over which the field varies. Its own gravitational back-reaction is negligible: for a defect of proton mass and size $R \sim 1\,\text{fm}$, $GM/(Rc^2) \approx 1 \times 10^{-39}$, so the deficits it induces in its own cells, and any feedback on its verification cost, are smaller than unity by that factor. The point-particle action of Proposition 2 is therefore the leading term of a multipole expansion whose corrections are computable and small, not an assumption that the defect has no structure.

5. Newton's Constant

The SSM fixes G independently, through its area law: one bit of entanglement per bond cell, matched to the Bekenstein–Hawking entropy, gives $G = L_f^2/(4\ln 2)$ [18]. The bonds of the spatial FCC slice are the D_4 roots with no time component, so L_f is also the D_4 nearest-neighbor distance. Equation (7) must agree with this value. Two inputs are needed: the cutoff and the field content.

The cutoff.

We fix Λ by mode counting rather than by hand, requiring one mode per lattice site per field component. For D_4 with nearest-neighbor distance L_f, the volume per site is $L_f^4/2$. Two identifications are natural. If the heat-kernel mode density at the cutoff, $(4\pi\Lambda^{-2})^{-2}$, equals the site density, then $\Lambda L_f = (32\pi^2)^{1/4} = 4.216$. If instead the momentum ball $|p| < \Lambda$ holds one mode per site, as in a Debye cutoff, then $\Lambda^4/32\pi^2 = 2/L_f^4$ and $\Lambda L_f = (64\pi^2)^{1/4} = 5.013$. The second is compatible with our proper-time coefficient, because the quadratic divergence has the same coefficient, $\Lambda^2/16\pi^2$, in proper-time and sharp-momentum regularization. The area law then requires

$$C_{\text{required}} = \frac{48\pi\ln 2}{(\Lambda L_f)^2} = 5.88\ \text{(heat-kernel density)}, \qquad 4.16\ \text{(Debye count)}. \tag{9}$$

The spread between the two measures the scheme dependence of the comparison.

The content.

We take the SSM's matter content to be three generations, each a Spin(10) spinor **16**, which contains one Standard Model generation and a right-handed neutrino [29,30]. The SSM program proposes that the three generations come from the triality of the D_4 cell, but this is not yet derived, and we treat the content as an input. Table 4 evaluates Equation (3) for this content and for alternatives. The field masses do not enter: they shift C by amounts of order $m^2/\Lambda^2 \lesssim 10^{-34}$.

Table 4. The coefficient C of Equation (3) and the ratio of the induced to the area-law Newton constant under the two mode-count cutoffs, which require $C = 5.88$ and $C = 4.16$. The 16 real scalars of the left–right model are a bidoublet and two doublets. In Pati–Salam, those doublets lie in $\chi_L = (\mathbf{4}, \mathbf{2}, \mathbf{1})$ and $\chi_R = (\mathbf{4}, \mathbf{1}, \mathbf{2})$, 16 real scalars each, with the bidoublet $\Phi = (\mathbf{1}, \mathbf{2}, \mathbf{2})$.

		$G_{\mathrm{ind}}/G_{\mathrm{area}}$	
Field Content	C	**Heat-Kernel**	**Debye**
Standard Model (45 Weyl, 12 gauge, minimal Higgs)	1	5.88	4.16
three **16** (48 Weyl), 12 gauge, minimal Higgs	4	1.47	1.04
three **16**, 12 gauge, conformal Higgs ($\xi = \frac{1}{6}$)	0	no induced G	
left–right: 15 gauge, 48 Weyl, 16 real scalars	4	1.47	1.04
Pati–Salam: 21 gauge, 48 Weyl, bidoublet $+ \chi_R$ (24 real scalars)	-12	negative G	
Pati–Salam: 21 gauge, 48 Weyl, bidoublet $+ \chi_L + \chi_R$ (40 real scalars)	4	1.47	1.04

For the SSM's content, the induced Newton constant has the right sign and agrees with the area-law value to within a factor 1.5 under either cutoff, 1.47 and 1.04, with no adjustable parameter (Figure 1b). The comparison also constrains content. Pati–Salam with the scalars $\Phi + \chi_R$ induces a negative Newton constant, while its left–right-symmetric completion $\Phi + \chi_L + \chi_R$ gives $C = 4$, the same as the left–right model. A conformally coupled Higgs induces no gravity, and the Standard Model without right-handed neutrinos underproduces it by a factor 4–6.

Two cautions keep this in proportion. First, $C = 4$ is a near-cancellation, $48 + 4 - 48$, between terms of order fifty, which we quantify next. The sign and the order-one agreement are the robust content; the precise ratio is scheme-dependent, as the two cutoffs show. Second, either mode count is a principled identification, not a derivation, of how a continuum regulator relates to the lattice spacing.

Sensitivity of the cancellation.

The cancellation is not technically natural: no symmetry ties the fermion and gauge-field contributions together, as supersymmetry would. Two kinds of perturbation must be distinguished. Interactions correct each species' quadratic coefficient at relative order $g^2/16\pi^2$, which, for gauge and Yukawa couplings near the Planck scale ($g \lesssim 0.6$), is $\approx 2 \times 10^{-3}$; summed over contributions of total magnitude about 100, this moves C by at most about 0.5, inside the window of A Gravity–Content Budget Section. Running below the cutoff does not enter, since C counts the fields present, not their couplings. The sensitive perturbation is a species-dependent cutoff. Giving each spin its own cutoff $\Lambda_s = \Lambda(1 + \epsilon_s)$ multiplies its contribution by $(1 + \epsilon_s)^2$, so that $\partial C/\partial \epsilon = 8$, 96, and -96 for the scalars, fermions, and gauge fields. Table 5 shows the effect of a relative mismatch $\Delta = \epsilon_f - \epsilon_v$ between the fermion and gauge-field cutoffs. The window $2.8 \lesssim C \lesssim 8.8$ holds for $-1.3\% \leq \Delta \leq +5.0\%$, and G stays positive for $\Delta > -4.2\%$. Uncorrelated variations are much milder: if each of the 64 fields receives its own cutoff with a random spread of 2% (5%), then $C = 4.0 \pm 0.6$ (± 1.6), inside the window in 98% (79%) of draws (`cutoff_asymmetry.py`). In the SSM, the cutoffs are equal for a structural reason: every field is counted with one mode per lattice site per component, because all fields live on the same lattice. That is a property of the model, not a symmetry protecting the result, so the agreement of the two values of G is a percent-level statement about the equality of the cutoffs of different spins. That is what makes it a test: a short-distance completion that treated fermions and gauge fields differently by more than a few percent would remove the agreement.

Table 5. Sensitivity of C and of $G_{\text{ind}}/G_{\text{area}}$ to a mismatch Δ between the fermion and gauge-field cutoffs, split symmetrically, for the SSM's content (three **16**, 12 gauge fields, minimal Higgs).

		$G_{\text{ind}}/G_{\text{area}}$	
$\Delta = \epsilon_f - \epsilon_v$	C	Heat-Kernel	Debye
−4%	0.16	36.8	26.0
−2%	2.08	2.83	2.00
−1%	3.04	1.93	1.37
0	4.00	1.47	1.04
+1%	4.96	1.19	0.84
+2%	5.92	0.99	0.70
+5%	8.80	0.67	0.47
+10%	13.60	0.43	0.31

A Gravity–Content Budget

The comparison can be read the other way. The SSM fixes Newton's constant twice and independently: through the area law, from black-hole entropy, and through the induced action, from the vacuum fluctuations of every field lighter than the cutoff. Requiring the two to agree confines C to a window. Taking the two mode counts, $C = 4.16$ and 5.88, and widening by their factor-1.5 spread gives $2.8 \lesssim C \lesssim 8.8$. Every field below the Planck scale enters, discovered or not; a field of mass m counts fully up to corrections of order m^2/Λ^2, which is 10^{-6} even at 10^{16} GeV. Table 6 tests candidate physics against the window.

Table 6. The gravity–content budget: Candidate field contents against the window $2.8 \lesssim C \lesssim 8.8$ required for the induced and area-law Newton constants to agree. The MSSM row counts 96 sfermion and 8 Higgs real scalars and $48 + 12 + 4$ Weyl fermions; minimal SU(5) counts 24 gauge bosons, 34 real scalars, and 45 Weyl fermions.

Field Content	C	Verdict
SM, three **16** (with ν_R), minimal Higgs	4	allowed
+ QCD axion	5	allowed
+ second Higgs doublet	8	allowed (marginal)
+ Z' gauge boson, no new scalars	0	excluded: no induced G
SM without ν_R	1	excluded: G 4–6× too strong
one or two generations	$-28, -12$	excluded: negative G
four generations	20	excluded: G 3–5× too weak
MSSM	120	excluded: G 20–29× too weak
MSSM, scalars conformally coupled	16	excluded: G 3–4× too weak
minimal SU(5)	−17	excluded: negative G
Higgs inflation ($\xi \sim 10^4$)	$\approx -2 \times 10^5$	excluded: negative G

Pati–Salam illustrates how the window acts on a scalar sector. With 21 gauge fields, 48 Weyl fermions, and N_s minimally coupled real scalars, $C = N_s - 36$, so the window requires $39 \leq N_s \leq 44$. The bidoublet Φ with χ_R ($N_s = 24$) leaves G negative; the left–right-symmetric sector $\Phi + \chi_L + \chi_R$ ($N_s = 40$) gives $C = 4$ and is allowed; Φ with a $(\mathbf{10}, \mathbf{1}, \mathbf{3})$ triplet Δ_R ($N_s = 68$) gives $C = 32$, a G five to eight times too weak. Gauged Spin(10), with 45 gauge fields, needs $135 \leq N_s \leq 140$: the sector $\mathbf{10}_H + \mathbf{16}_H + \mathbf{45}_H$ (97 real scalars) gives a negative G, and $\mathbf{10}_H + \overline{\mathbf{126}}_H + \mathbf{45}_H$ (317) a G thirty to forty-five times too weak (`budget.py`). An enlarged scalar sector does not reintroduce the shear instability of Section 3. That instability belongs to lattice-regulated bosons; under Postulate 2, every species, scalars included, is regulated covariantly and contributes no shape term, whatever the number of scalars. What additional scalars change is C, each by $1 - 6\xi$, and the cosmological coefficient, each by one bosonic degree of freedom.

Read as predictions, the budget says the following, each falsifiable. Right-handed neutrinos exist. The number of generations is three: with fewer, the gauge bosons outweigh the fermions and G is negative; with four or more, gravity is several times too weak. There are no supersymmetric partners below the Planck scale, whose scalars would make gravity twenty to thirty times too weak, or three to four times even if conformally coupled. The Higgs couples to curvature with $-0.20 \lesssim \xi \lesssim 0.05$, which excludes Higgs inflation. Grand unification below the Planck scale with a minimal scalar sector is excluded, minimal SU(5) by the sign of G and gauged Spin(10) unless its scalar sector has 135–140 real scalars, so in the SSM, Spin(10) most naturally organizes the fermions rather than acting as a gauge symmetry. Partial unification is not excluded: Pati–Salam with a left–right-symmetric scalar sector is allowed. A new gauge boson requires at least three new real scalars. And the room left for undiscovered physics is finite, $-1.2 \lesssim \Delta C \lesssim 4.8$ above the Standard Model: enough for an axion, a second Higgs doublet, or a few sterile fermions, but not much more.

The exclusions by sign or by a factor of three or more hold under either mode count and do not depend on the tolerance; the marginal cases, such as a second Higgs doublet, do. The near-cancellation in C applies here as in Table 4, scalars enter through $\sum_i (1 - 6\xi_i)$ rather than their number, and graviton loops are omitted. That induced gravity constrains field content is known qualitatively, since gauge fields enter with the opposite sign; what the SSM adds is an independent value of G, which turns a sign condition into a numerical window.

6. Consistency

With the D_4 Regge sector.

On the closed D_4 complex the Regge action's quadratic and cubic terms equal Fierz–Pauli and Einstein–Hilbert exactly, and its static field gives the Newtonian normalization and $\beta = \gamma = 1$ [4]. Those results took the Regge action as input; here it is an output, and they carry over. The coefficient of t in the heat trace is $\frac{1}{6}\int \sqrt{g}R$ for any metric, so the induced action equals the Regge action at two derivatives to all orders in the metric perturbation, and differs from it only at four derivatives. Every result of Reference [4] is a two-derivative statement, so each holds for the induced action, with $G = G_{\mathrm{ind}}$. The chain is closed: the vacuum fluctuations induce Einstein–Hilbert, which, on the lattice, is the Regge action, which at long wavelength is Einstein–Hilbert again.

With the cosmological constant.

The a_0 term of Equation (1) is a cosmological term of order Λ^4 times the difference of bosonic and fermionic degrees of freedom, 28 against 96 for the SSM's content (three copies of the **16**, the Standard Model gauge group, and a minimal Higgs). It requires the self-tuning of a self-bound vacuum [31], in which the gravitating combination is $-P$ and vanishes in equilibrium; the ocean picture is natural for this mechanism, since a self-bound medium adjusts to zero pressure. The mechanism acts through a density, so it can cancel a vacuum energy that depends on volume but not one that depends on shape. That is why the shape terms of Section 3 are fatal for lattice-regulated fields, and why Postulate 2 matters here too: under it, no shape term arises, and the vacuum energy that remains is exactly the kind self-tuning can remove.

With the matter coupling.

Defects source the geometry through their center-of-mass worldlines with the action of Proposition 2, whose static limit is the coupling assumed in Reference [4]; the vacuum fluctuations respond to the geometry. The far field depends only on the total mass, by the Newtonian normalization of Reference [4], so the internal structure of a defect does not enter. Because the stabilizer vacuum has exactly zero energy for any couplings (Section 3),

a defect's verification cost is its whole energy, with no vacuum offset to subtract, so the mass that sources the geometry is unambiguous.

With Lorentz invariance.

The induced action is covariant, but the lattice geometry it acts on is not: the Regge action on D_4 carries anisotropic corrections at relative order $(ka)^2$, tabulated for the static field in Reference [4]. Lorentz violation therefore enters only through the lattice geometry, suppressed by $(E/E_P)^2$ at energy E, and not through the vacuum fluctuations themselves.

With the lattice no-go.

Section 3 showed that lattice-regulated fields induce a graviton mass. Under Postulate 2, the shape terms vanish by symmetry, and no balance between bosons and fermions is needed for the graviton to stay massless. Balance still enters, through C and the cosmological term, but as a condition on magnitudes, not on covariance.

7. Limitations and Status

Table 7 grades each claim. The main limitations are these.

Table 7. Status of the paper's claims, in the order of the paper: premises, the no-go, the derivations, and their consistency.

Claim	Status
vacuum fluctuations exist now	measured [11–13]
fluctuations predate spacetime (Postulate 1)	premise, not directly testable
saturation rule: no new bonds inside space	kissing-number theorems [16,17]
first-triangle account of crystallization	interpretation
lattice has no appreciable stiffness of its own (Section 4.4)	SSM result; required by Section 3
stabilizer sector induces no action	exact (commuting checks)
lattice-regulated fields induce a graviton mass (Table 1)	computed
softened lattice cutoff: excess falls only as $(\Lambda L_f)^2$ (Table 2)	computed
Sakharov coefficients, Equation (3)	standard heat kernel, rederived
$\int \sqrt{g}R = 2\sum A\delta$ on piecewise-flat geometry	exact identity
conical vertex coefficient, Equation (5)	computed from the exact spectrum
Λ^2 term additive over intersecting hinges	derived (heat-kernel structure); exact orbifold check
Postulate 2 (covariance)	assumed
Regge action induced, Proposition 1	derived, given Postulate 2
Postulate 3 (ticks are proper time)	assumed
verification cost couples as rest mass, Proposition 2	derived, given Postulate 3
field content: three **16**, scalar sector	input, not derived in the SSM
gravity–content budget (Table 6)	follows from the two values of G; window tolerance-dependent
G_{ind} against the area law	sign and order of magnitude robust; factor 1.5 scheme-dependent
cancellation in C under cutoff mismatch	computed: window holds for $-1.3\% \leq \Delta \leq 5\%$; not technically natural
two-derivative D_4 results hold for the induced action	follows (Section 6)
Lorentz violation only through the lattice geometry	follows (Section 6)
cosmological term canceled	imported self-tuning [31]
covariance from lattice dynamics	open
Lorentzian signature, higher loops, graviton loops	not computed; estimated (Section 7)

The postulates.

Postulate 1 is the model's premise: that the fluctuations persist is observed, but that they predate spacetime is not directly testable. Postulate 2 is assumed. The derivation of the action moves the assumption from the Regge action to the covariance of the vacuum fluctuations, which is better grounded, since the observed vacuum is Lorentz invariant, but it is not derived from the lattice. Its weakest joint is that it asks for a regulator covariant in form but set at a scale the lattice defines; how a Lorentz-invariant cutoff comes to sit at the lattice spacing is not explained here. Section 2 states what the postulate does and does not require; a dynamical mechanism for it is the paper's principal open problem. That the lattice has no appreciable stiffness of its own (Section 4.4) is taken from the SSM, not rederived here, though Section 3 shows it is required. Postulate 3, which identifies the count of verification ticks with the proper time of the Regge geometry, is the one input of the source derivation; it is natural in a model that defines time by those ticks, but it is assumed.

Newton's constant.

The value of G_{ind} is reliable to a factor of a few, so the agreement to within a factor 1.5 in Section 5 is partly fortuitous; its robust content is the sign and the order of magnitude. The two mode counts of Section 5 differ by a factor 1.41 in G, and C is a near-cancellation, sensitive to the relative cutoffs of different species. The field content is an input: neither the three generations nor the scalar sector is yet derived in the SSM, and each real scalar changes C by one. The gravity–content budget of A Gravity–Content Budget Section inherits these caveats, and its marginal cases depend on the chosen tolerance.

Signature, loop order, and back-reaction.

The induced action is computed in Euclidean signature at one loop. The heat-kernel coefficients are local short-distance quantities, so G_{ind}, the coefficient of the local term $\int \sqrt{g}\, R$, is unchanged by continuation to Lorentzian signature, as is standard in induced gravity [6]; on the lattice, the continuation is the Lorentzian Regge action, in which the deficits at timelike hinges become boost parameters [32]. A direct Lorentzian computation of the conical term is not performed. Higher matter loops correct C by at most about 0.5 (Section 5). The treatment is semiclassical: the geometry responds to the fluctuations' effective action, which is what varying the induced action computes. The singular curvature at a hinge does not require a small-curvature expansion, since the conical term is computed exactly at one loop for every cone angle tested, up to a deficit of 240°; the expansion made is in the deficits of different hinges, which are small in the weak field. Graviton loops are not computed. In induced gravity, the graviton is not a fundamental field of the ocean, but the edge lengths do fluctuate, and their loop renormalizes $1/G$ by a quadratically divergent amount whose coefficient depends on the gauge and the parametrization of the metric. Its size in this framework is not known; it is not part of the present result, and it adds to the order-one uncertainty of the comparison.

The cosmological term.

The paper does not solve the cosmological-constant problem. The a_0 term is the same as in any theory of induced gravity, and its cancellation is imported from self-tuning [31], to show that the derived action is consistent with a vanishing cosmological term, not as a result. What the derivation contributes is the precondition any density-type solution needs: under Postulate 2, the vacuum energy depends on volume only, not on shape (Section 3).

Vacancy boundaries.

Whether the ocean restitches the boundary of a vacancy faster than the vacancy evaporates concerns the SSM's black-hole sector [18], not the saturated bulk to which the derivation applies. The induced Regge action holds wherever the lattice is saturated; whether a vacancy grows or heals depends on stitching kinetics that this paper does not treat, and no result here depends on the answer.

What is omitted.

The fluctuations of the lattice's own geometry beyond one loop are omitted. The $O(\delta^2)$ hinge corrections are computed for a scalar at an isolated hinge only, and the phase per operation φ_0 in Proposition 2 is fixed by the SSM's calibration rather than derived. The account of the ocean before the lattice is interpretation, not used in either derivation.

8. Conclusions

The vacuum fluctuations are measured, and in the Selection–Stitch Model's interpretation, they are older than space: the lattice and its defects are made of them, and the existing lattice excludes new stitching by the rule that built it. Gravity then need not be postulated as Regge calculus. If the fluctuations around the lattice are covariant, integrating them out induces the Einstein–Hilbert action, which, on the lattice's piecewise-flat geometry, is exactly the Regge action; the conical heat kernel confirms this on the hinge itself, with a curvature-squared correction of relative size $\delta/4\pi$. A defect's verification cost, counted in the ticks that define time, couples as a rest mass, so it is the source of that curvature and the equivalence principle follows. The fluctuations cannot instead be the lattice's own fields, whose induced vacuum energy depends on the shape of the lattice and gives the graviton a mass. The induced Newton constant, with the cutoff set by the lattice's mode density and three generations of the Spin(10) spinor taken as the SSM's content, has the right sign and agrees with the SSM's area-law value to within a factor of 1.5 under either mode count, and the agreement constrains everything below the Planck scale: it admits three generations with right-handed neutrinos and excludes supersymmetry, a fourth generation, minimal grand unification, and Higgs inflation. The lattice is what bends, the defects are what bend it, and the vacuum's fluctuations are what resist. Two questions remain open. The principal one is whether the lattice dynamically permits the covariance of the fluctuations, which the derivation assumes. The other is where that picture meets its own boundary: whether the fluctuations restitch the edge of a vacancy faster than it evaporates.

Funding: This research received no external funding.

Data Availability Statement: The original data presented in the study are openly available in the archive ocean_regge.zip at https://github.com/raghu91302/ssmtheory, (accessed on 21 October 2026), (Appendix B).

Acknowledgments: The author thanks the three reviewers, whose comments improved the treatment of the covariance postulate, the intersecting hinges, and the sensitivity of the induced Newton constant. During the preparation of this work, the author used Claude Opus 5.5 (Anthropic, San Francisco, CA, USA) to write and run the verification and analysis scripts, generate the figures, analyze the numerical results, and draft and edit the manuscript text and LaTeX source. The author has reviewed and edited the output and takes full responsibility for the content of this publication.

Conflicts of Interest: Raghu Kulkarni is an employee of SSMTheory Group, IDrive Inc. The views expressed in this article are those of the author and do not necessarily represent the views of IDrive Inc.

Appendix A. Heat-Kernel Coefficients

For $\mathcal{D} = -(\nabla^2 + E)$ acting on a bundle of rank n, $a_1 = \mathrm{tr}(E) + nR/6$. A real scalar with coupling ξR has $E = -\xi R$, so $a_1 = (\frac{1}{6} - \xi)R$. A Dirac fermion has $\not{D}^2 = -\nabla^2 + R/4$ on four components, so $a_1 = 4(\frac{1}{6} - \frac{1}{4})R = -\frac{1}{3}R$, and its effective action $-\frac{1}{2}\log\det\not{D}^2$ carries $s = -1$; a Weyl fermion is half of this. A gauge field in Feynman gauge has $\mathcal{D} = -\nabla^2 + \mathrm{Ric}$ on vectors, so $a_1 = \frac{4}{6}R - R = -\frac{1}{3}R$, and its two Faddeev–Popov ghosts subtract $2 \times \frac{1}{6}R$, giving $-\frac{2}{3}R$ with $s = +1$. Relative to a minimal real scalar ($a_1 = \frac{1}{6}R$, $s = +1$), the contributions to C are $1 - 6\xi$, 2, 1, and -4 for a scalar, Dirac fermion, Weyl fermion, and gauge field. The cosmological coefficient $a_0 = \mathrm{tr}\,1$ counts degrees of freedom with the sign s: a real scalar counts 1, a gauge field $4 - 2 = 2$ after its ghosts, and a Weyl fermion 2 with the opposite sign. For the SSM's content (three copies of the **16**, the Standard Model gauge group, and a minimal Higgs), this gives $4 + 12 \times 2 = 28$ bosonic against $48 \times 2 = 96$ fermionic degrees of freedom.

Appendix B. Reproducibility

The archive `ocean_regge.zip` contains the scripts for every number in this paper. `cone_heat.py` computes the Bessel spectra of cone-disks and fits the heat-kernel constant (Table 3); `budget.py` gives Table 6; `newton.py` evaluates Equation (3) under both mode-count cutoffs (Table 4); `make_figs.py` draws Figure 1. The lattice results of Table 1 are reproduced by `induced_k0.py` (scalar), `rotor_k0.py` (gauge field), `fermion_k0.py` (Wilson–Dirac), `geometric_control.py` (continuum kinetic tensor), and `root_p.py` and `rotor_p2.py` (the exponents p^*). `cutoff_asymmetry.py` gives Table 5 and the per-species jitter statistics, and `soft_cutoff_covariance.py` gives Table 2, and `orbifold_hinges.py` computes the exact heat traces of the intersecting-hinge orbifolds of Section 4.3; `budget.py` also evaluates the Pati–Salam scalar sectors. All scripts require only Python 3 with NumPy, SciPy, and Matplotlib, and the archive's `README.md` gives the command for each.

References

1. Kulkarni, R. A 67%-rate CSS code on the FCC lattice: [[192,130,3]] from weight-12 stabilizers. *arXiv* **2026**, arXiv:2603.20294.
2. Kulkarni, R. Matter as incomplete crystallization: Quark charges, color confinement, and the proton mass from a single extra node in the vacuum lattice. *Phys. Open* **2026**, *27*, 100423. [CrossRef]
3. Regge, T. General relativity without coordinates. *Nuovo Cim.* **1961**, *19*, 558. [CrossRef]
4. Kulkarni, R. Regge calculus on the D_4 lattice through second order: Exact identities and the post-Newtonian static field. *Zenodo* **2026**. [CrossRef]
5. Sakharov, A.D. Vacuum quantum fluctuations in curved space and the theory of gravitation. *Gen. Relativ. Gravit.* **2000**, *32*, 365. [CrossRef]
6. Visser, Sakharov's induced gravity: A modern perspective. *Mod. Phys. Lett. A* **2002**, *17*, 977–991. [CrossRef]
7. Lamb, W.E.; Retherford, R.C. Fine structure of the hydrogen atom by a microwave method. *Phys. Rev.* **1947**, *72*, 241. [CrossRef]
8. Bethe, H.A. The electromagnetic shift of energy levels. *Phys. Rev.* **1947**, *72*, 339. [CrossRef]
9. Welton, T.A. Some observable effects of the quantum-mechanical fluctuations of the electromagnetic field. *Phys. Rev.* **1948**, *74*, 1157. [CrossRef]
10. Casimir, H.B.G. On the attraction between two perfectly conducting plates. *Proc. Kon. Ned. Akad. Wetensch.* **1948**, *51*, 793.
11. Riek, C.; Seletskiy, D.V.; Moskalenko, A.S.; Schmidt, J.F.; Krauspe, P.; Eckart, S.; Eggert, S.; Burkard, G.; Leitenstorfer, A. Direct sampling of electric-field vacuum fluctuations. *Science* **2015**, *350*, 420. [CrossRef] [PubMed]
12. Benea-Chelmus, I.-C.; Settembrini, F.F.; Scalari, G.; Faist, J. Electric field correlation measurements on the electromagnetic vacuum state. *Nature* **2019**, *568*, 202. [CrossRef] [PubMed]
13. Settembrini, F.F.; Lindel, F.; Herter, A.M.; Buhmann, S.Y.; Faist, J. Detection of quantum-vacuum field correlations outside the light cone. *Nat. Commun.* **2022**, *13*, 3383. [CrossRef] [PubMed]
14. Wilson, C.M.; Johansson, G.; Pourkabirian, A.; Simoen, M.; Johansson, J.R.; Duty, T.; Nori, F.; Delsing, P. Observation of the dynamical Casimir effect in a superconducting circuit. *Nature* **2011**, *479*, 376. [CrossRef] [PubMed]
15. Jaeger, G. Are virtual particles less real? *Entropy* **2019**, *21*, 141. [CrossRef] [PubMed]
16. Schütte, K.; van der Waerden, B.L. Das Problem der dreizehn Kugeln. *Math. Ann.* **1953**, *125*, 325. [CrossRef]

17. Musin, O.R. The kissing number in four dimensions. *Ann. Math.* **2008**, *168*, 1. [CrossRef]
18. Kulkarni, R. Black holes in the FCC selection–stitch model: Bekenstein–Hawking entropy, geometric evaporation, and primordial-black-hole signatures. *Eur. Phys. J. Plus* **2026**, *141*, 916. [CrossRef]
19. Cheeger, J.; Müller, W.; Schrader, R. On the curvature of piecewise flat spaces. *Commun. Math. Phys.* **1984**, *92*, 405. [CrossRef]
20. Cheeger, J. Spectral geometry of singular Riemannian spaces. *J. Differ. Geom.* **1983**, *18*, 575. [CrossRef]
21. Bombelli, L.; Henson, J.; Sorkin, R.D. Discreteness without symmetry breaking: A theorem. *Mod. Phys. Lett. A* **2009**, *24*, 2579. [CrossRef]
22. Abbott, R.; Abe, H.; Acernese, F.; Ackley, K.; Adhikari, N.; Adhikari, R.X.; Adkins, V.K.; Adya, V.B.; Affeldt, C.; Agarwal, D. Tests of general relativity with GWTC-3. *Phys. Rev. D.* **2025**, *112*, 084080. [CrossRef]
23. Wilson, K.G. Confinement of quarks. *Phys. Rev. D.* **1974**, *10*, 2445. [CrossRef]
24. Vassilevich, D.V. Heat kernel expansion: User's manual. *Phys. Rep.* **2003**, *388*, 279–360. [CrossRef]
25. Dowker, J.S. Quantum field theory on a cone. *J. Phys. A* **1977**, *10*, 115. [CrossRef]
26. Fursaev, D.V.; Solodukhin, S.N. On the description of the Riemannian geometry in the presence of conical defects. *Phys. Rev. D.* **1995**, *52*, 2133–2143. [CrossRef] [PubMed]
27. Kabat, D. Black hole entropy and entropy of entanglement. *Nucl. Phys. B* **1995**, *453*, 281–299. [CrossRef]
28. Barvinsky, A.O.; Vilkovisky, G.A. Covariant perturbation theory (II): Second order in the curvature. General Algorithms. *Nucl. Phys. B* **1990**, *333*, 471. [CrossRef]
29. Georgi, The state of the art—Gauge theories. *AIP Conf. Proc.* **1975**, *23*, 575. [CrossRef]
30. Fritzsch, H.; Minkowski, P. Unified interactions of leptons and hadrons. *Ann. Phys.* **1975**, *93*, 193. [CrossRef]
31. Klinkhamer, F.R.; Volovik, G.E. Self-tuning vacuum variable and cosmological constant. *Phys. Rev. D.* **2008**, *77*, 085015. [CrossRef]
32. Sorkin, R.D. Time-evolution problem in Regge calculus. *Phys. Rev. D.* **1975**, *12*, 385. Erratum in *Phys. Rev. D.* **1981**, *23*, 565. [CrossRef]

Disclaimer/Publisher's Note: The statements, opinions and data contained in all publications are solely those of the individual author(s) and contributor(s) and not of MDPI and/or the editor(s). MDPI and/or the editor(s) disclaim responsibility for any injury to people or property resulting from any ideas, methods, instructions or products referred to in the content.